Heliyon 10 (2024) e25763

Contents lists available at ScienceDirect

Heliyon

journal homepage: www.cell.com/heliyon

Research article

Diphenyl ethers from the cultured lichen mycobiont of *Graphis handelii* Zahlbr

Thi-Minh-Dinh Tran [a,b,*], Chanat Aonbangkhen [c], Thuc-Huy Duong [d], Thu-Hoang-Mai Nguyen [d], Minh-Truong-Tho Ho [d], Warinthorn Chavasiri [c,e], Sutthida Wongsuwan [f], Jaruwan Chatwichien [f], Thi-Phi Giao Vo [g], Ngoc-Hong Nguyen [h], Duangnapa Kiriwan [i], Kiattawee Choowongkomon [b,i,**]

[a] *Department of Biology, Ho Chi Minh City University of Education, 280 an Duong Vuong Street, District 5, Ho Chi Minh City, 748342, Viet Nam*
[b] *KU Institute for Advanced Studies, Kasetsart University, Bangkok, 10900, Thailand*
[c] *Center of Excellence in Natural Products Chemistry, Department of Chemistry, Chulalongkorn University, Pathumwan, Bangkok, 10330, Thailand*
[d] *Department of Chemistry, Ho Chi Minh City University of Education, 280 an Duong Vuong Street, District 5, Ho Chi Minh City, 748342, Viet Nam*
[e] *Nanotec-CU Center of Excellence on Food and Agriculture, Department of Chemistry, Chulalongkorn University, Bangkok, 10330, Thailand*
[f] *Program in Chemical Sciences, Chulabhorn Graduate Institute, Chulabhorn Royal Academy, Bangkok, 10210, Thailand*
[g] *University of Science, Vietnam National University Ho Chi Minh City, Ho Chi Minh City, Viet Nam*
[h] *CirTech Institute, HUTECH University, 475 A Dien Bien Phu Street, Binh Thanh District, Ho Chi Minh City, Viet Nam*
[i] *Department of Biochemistry, Kasetsart University, Bangkok, Thailand*

A R T I C L E I N F O

Keywords:
Cultured lichen mycobiont
Graphis handelii
Depsidone
Handelone
Alpha-glucosidase inhibition
M^{pro} inhibition

A B S T R A C T

Purpose: Cultured lichen mycobionts are valuable sources of new natural compounds. Mycobiont of *Graphis handelii* growing in Vietnam was isolated, cultivated and chemically investigated. The crude extract of this cultured mycobiont showed potent alpha-glucosidase inhibition with an IC_{50} value of 50 μg/mL.

Methods: Multiple chromatographic methods were applied to the extract to isolate compounds. The combination of Nuclear Magnetic Resonance analysis and high-resolution mass spectroscopy determined their chemical structures. Electrophilic bromination/chlorination was applied to obtain new derivatives using $NaBr/H_2O_2$ and $NaCl/H_2O_2$ reagents. Compounds were evaluated for enzyme inhibitory activities, including alpha-glucosidase inhibition, HIV-1 reverse transcriptase inhibition, SARS-CoV-2 main protease (M^{pro}) inhibition, anti-inflammatory activity, and cytotoxicity against several cancer cell lines. A molecular docking study for *anti*-SARS-CoV-2 was conducted to understand the inhibitory mechanism.

Results: A new diphenyl ether, handelone (**1**) and a known compound xylarinic acid A (**2**) were isolated and elucidated. Four synthetic products 6′-bromohandelone (**1a**), 2′-bromohandelone (**1b**), 2′,6′-dibromohandelone (**1c**), and 2′,6′-dichlorohandelone (**1d**) were prepared. Compound **1** showed good activity against M^{pro} with an IC_{50} value of 5.2 μM but it showed weak or inactive activity in other tests. Other compounds were inactive in all assays.

Conclusion: A new compound, handelone (**1**) was isolated from the cultured mycobiont of *Graphis handelii*. From these compounds, four new derivatives were prepared. Compound **1** showed good

* Corresponding author. Department of Biology, Ho Chi Minh City University of Education, 280 An Duong Vuong Street, District 5, Ho Chi Minh City, 748342, Viet Nam.
** Corresponding author. KU Institute for Advanced Studies, Kasetsart University, Bangkok, 10900, Thailand.
E-mail addresses: dinhttm@hcmue.edu.vn (T.-M.-D. Tran), fsciktc@ku.ac.th (K. Choowongkomon).

https://doi.org/10.1016/j.heliyon.2024.e25763
Received 19 November 2023; Received in revised form 1 February 2024; Accepted 1 February 2024
Available online 7 February 2024

activity against M^{pro} with an IC_{50} value of 5.2 μM but it showed weak or inactive activity in other tests. Other compounds were inactive in all assays.

1. Introduction

Cultured lichen mycobionts are believed to be valuable sources of naturally occurring molecules with unique scaffolds [1–7]. Cultured mycobionts derived from several *Graphis* species were chemically investigated such as *G. scripta* [8], *G. vertitoides* [1], *G. tetraloculari* [9], *G. proserpens*, *G. apriens*, *G. handelii*, *G. awaensis* [4], *G. rikuzensis* [10], and two others *Graphis* sp. growing in Vietnam [10,11]. An abundance of skeletons including 6*H*-dihydro[*b*,*d*]pyran-6-one derivatives [5], isocoumarins [12], diphenyl ethers [11], isochromene derivatives [12], and eremophillane-type sesquiterpenoids [10] were reported. Up to now, there is only one chemical investigation on cultured mycobiont of *G. handelii* which reported the presence of graphenone [3]. In the continuing study on Vietnamese lichen mycobionts [10,13,14], chemical investigations were performed on cultured mycobiont of the lichen *Graphis handelii*. In this study, we successfully isolated and elucidated the structure of a new diphenyl ether, handelone (**1**), together with a known compound xylarinic acid A (**2**) [15]. Compound **1** was selected for halogenation to obtain products 6′-bromohandelone (**1a**), 2′-bromohandelone **(1b)**, 2′,6′-dibromohandelone **(1c)**, and 6′-chlorohandelone (**1d**). The combination of Nuclear Magnetic Resonance analysis and high-resolution mass spectroscopy determined the chemical structures of compounds **1** and **1a**-**1d**. They were evaluated for alpha-glucosidase inhibition, HIV-1 reverse transcriptase inhibition, M^{pro} inhibition, anti-inflammatory activity, and cytotoxicity against several cancer cell lines.

2. Results and discussion

2.1. Structural elucidation of compound 1

Compound **1** was obtained as a white amorphous powder. The molecular formula of **1** was deduced as $C_{17}H_{18}O_7$ by the deprotonated molecular ion peak at *m/z* 315.0867 (calcd. for $[C_{17}H_{18}O_7–H_2O–H]^-$, 315.0868) in HRESI mass spectrum (Fig. S3). The ^1H NMR spectrum showed three aromatic protons [δ_H 6.55 (1H, brs, H-4′), 6.52 (1H, s, H-3), 6.39 (1H, brs, H-6′)], two methoxy groups [δ_H 3.84 (3H, s, 3′-OCH_3) and 3.80 (3H, s, 4-OCH_3)], and two methyl groups [δ_H 2.23 (3H, s, H_3-8) and 2.18 (3H, s, H_3-7′)]. The JMOD spectrum in accordance with HSQC spectrum exhibited 17 carbons resonances attributable to a carbonyl group (δ_C 167.9, C-7), three methine carbons (δ_C 109.8, 109.2, and 99.2), two methyl carbons (δ_C 21.2 and 12.3) and nine quaternary carbons (δ_C 153.3, 148.7, 143.7, 143.2, 134.3, 134.3, 129.7, 124.9, and 121.0). These spectroscopic data indicated that **1** was a phenolic compound having two benzene rings. In the so-called A-ring, H_3-8 (δ_H 2.18) gave ^3J HMBC correlations to carbons at δ_C 121.0 (C-1), 124.9 (C-6) and 134.3 (C-5), and ^4J HMBC correlations to carbons at δ_C 143.7 (C-2) and 153.3 (C-4) (see Fig. 2). The proton at δ_H 6.52 (H-3) gave HMBC cross peaks to four previously mentioned carbons, indicating the position of this proton in the A-ring. The methoxy group (δ_H 3.80) was located at C-4 due to a key HMBC correlation of this group to C-4. The carbonyl group was determined to be attached at C-1 based on a long-range HMBC correlation of H_3-8 to carbon at δ_C 167.9 (C-7). Combined, the chemical structure of the A-ring was defined. NMR data of **1** were highly similar to those of corynesidone E [16] (Table 1), indicating that compound **1** had the similar A-ring as corynesidone E. It indicated that **1** could be a diphenyl ether or a depsidone. The obvious difference is the chemical shift of C-2 (δ_C 143.7 in **1** vs. 156.4 in corynesidone E). The upfield chemical shift of C-2 suggested that **1** was a diphenyl ether which could be found in parmoethers A and B isolated from the lichen *Parmotrema tsavoense* [17].

In the B-ring, the methyl at δ_H 2.23 (H_3-7′) gave HMBC correlations to both methine carbons at δ_C 109.8 (C-6′) and 109.2 (C-4′), and both aromatic protons [δ_H 6.55 (1H, brs, H-4′) and 6.39 (1H, brs, H-6′)] gave a HMBC correlation to C-7′ (δ_C 21.2), indicating the connectivity through C-4′-C-5′-C-6′. The chemical shifts of the remaining carbons in the B-ring indicated that all of them were oxygenated, leading to two possible structures of **1** (**I** and **II**, Fig. S2). Comparison of the ^{13}C chemical shifts of these oxygenated carbons (C-1′, C-2′, C-3′) with those of isomoniliformine A [18] and dehydrodieugenol B [19] (Fig. S2) indicated the similar C-2′ chemical shifts of **1** and isomoniliformine A. It is noted that NMR data of **1** in different deuterated solvents (acetone-d_6, DMSO-d_6, and chloroform-*d*) gave the similar C-2′ chemical shift (δ_C 128.1–129.7, see Table S1, Fig. S2). This finding indicated that the most likely structure of **1** should be isomer **I**. To corroborate the chemical structure of **1**, two isomers **I** and **II** of compound **1** were optimized using the B3LYP/6-311g(d,p) method in Schrodinger's Jaguar software. The calculations were conducted under DFT theory, considering

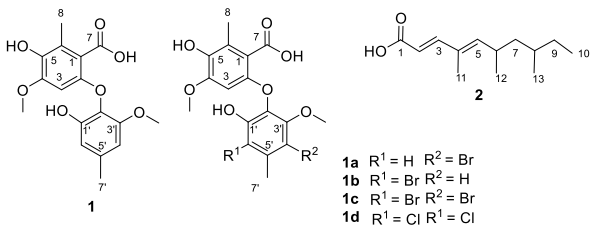

Fig. 1. Chemical structures of compounds **1**, **2**, and **1a-1d**.

Table 1
^{1}H (500 MHz) and ^{13}C (125 MHz) NMR data of compounds **1** and **1a-1d**.

No	1		1a		1 b		1c		1 d	
	δ_H[a] (multi., *J* in Hz)	δ_C[a]	δ_H[a] (multi., *J* in Hz)	δ_C[a]	δ_H[b] (multi., *J* in Hz)	δ_C[b]	δ_H[b] (multi., *J* in Hz)	δ_C[b]	δ_H[b] (multi., *J* in Hz)	δ_C[b]
1		121.0		113.0		119.4		120.1		116.5
2		143.7		142.0		141.0		140.6		143.5
3	6.52 (1H, s)	99.2	6.71 (1H, s)	98.9	6.51 (1H, s)	98.5	6.49 (1H, s)	98.4	6.52 (1H, s)	98.4
4		153.3		152.5		152.3		152.5		153.9
5		134.3		133.9		134.1		134.7		130.4
6		124.9		127.0		122.7		127.1		127.0
7		167.9		163.5		165.8		168.7		nd
8	2.18 (3H, s)	12.3	2.30 (3H, s)	13.3	2.40 (3H, s)	15.7	2.53 (3H, s)	15.7	2.45 (3H, s)	13.0
1′		143.2		142.5		140.3		145.1		142.7
2′		129.7		131.1		127.9		128.1		134.5
3′		148.7		145.1		146.4		144.4		145.1
4′	6.55 (1H, brs)	109.3		104.3	6.49 (1H, s)	108.6		108.7		122.1
5′		134.3		134.5		133.0		132.8		134.5
6′	6.39 (1H, brs)	109.8	6.65 (1H, s)	110.2		103.8		107.8		110.9
7′	2.23 (3H, s)	21.2	2.32 (3H, s)	21.6	2.40 (3H, s)	22.8	2.41 (3H, s)	22.8	2.28 (3H, s)	17.3
4–OCH_3	3.80 (3H, s)	55.6	3.87 (3H, s)	56.7	3.87 (3H, s)	56.6	3.91 (3H, s)	56.8	3.92 (3H, s)	57.0
3′–OCH_3	3.84 (3H, s)	55.8	3.90 (3H, s)	60.1	3.81 (3H, s)	56.8	3.85 (3H, s)	61.2	3.90 (3H, s)	61.5

Nd: not determined.
[a] Acetone-d_6.
[b] $CDCl_3$.

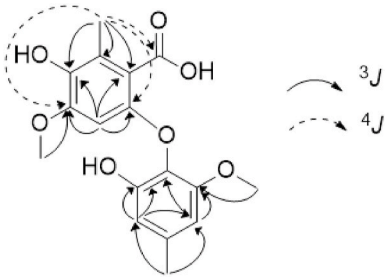

Fig. 2. Selected HMBC correlations of **1**.

NMR shielding constants in the gas phase [20,21]. Then, DP4 probability was applied to two isomers **I** and **II**, resulting in a 85.22 % probability in favor of isomer **I**. Altogether, the chemical structure of **1**, or handelone, was elucidated as shown in Fig. 1.

The elevated number of diphenyl ethers have been commonly found in lichen; nevertheless, these compounds rarely occurred in cultured mycobionts.

Halogenated substitution using sodium bromide/sodium chloride and hydroperoxide was conducted on **1** to provide products **1a-1d** (Scheme 1). This reaction was selected based on enhancing alpha-glucosidase inhibition of brominated derivatives from the previous report [22]. Synthetic products were identified using HRESIMS, 1D and 2D-NMR (Table 1).

2.2. Alpha-glucosidase inhibition

An evaluation of the crude extract and the fractions GR1-GR5 for their alpha-glucosidase inhibitory properties was performed (see Table 2). The activity of fraction GR1 was significantly higher than that of other fractions, as indicated by its IC_{50} value of 57.8 ± 0.7 μg/mL. Hence, this fraction was selected for further isolation to obtain compound **1**. The inhibitory effects of compounds **1** and **1a-1d** were assessed. It is unfortunate that they were inactive.

2.3. HIV-1 reverse transcriptase inhibition

Compounds **1** and **1a-1d** were screened for HIV-1 reverse transcriptase inhibition at the final concentration of 10 μM. Only compound **1** showed the inhibition percentage of 24.3% (see Table 3).

2.4. SARS-CoV-2 M^{pro} inhibition

Compounds **1** and **1a-1d** were screened for M^{pro} inhibition at the final concentration of 10 μM. The highest activity was displayed by compound **1** with the inhibition percentage of 70.7% (Table 4). Other compounds showed the inhibition below 50% (see Table 4).

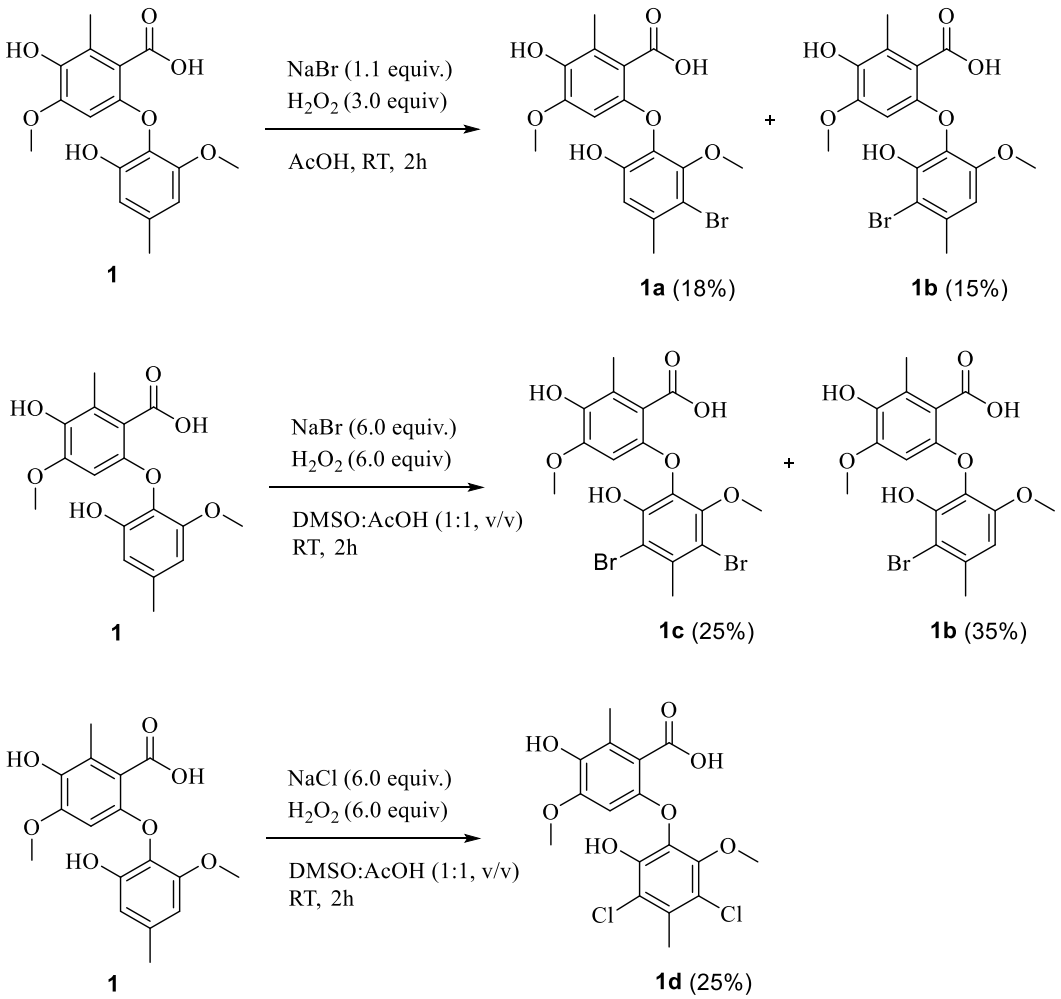

Scheme 1. General procedure from **1** to **1a-1d**.

Table 2
Alpha-glucosidase inhibition of the crude extract, fractions, and compound **1**.

Sample	IC_{50} (μg/mL)
Crude extract	50.0 ± 0.6
Fr. GR1	57.8 ± 0.7
Fr. GR2	nd
Fr. GR3	109.9 ± 1.1
Fr. GR4	nd
Fr. GR5	nd
1	nd
1a-1d	nd
Acarbose	360.0 ± 3.1

nd: not determined.

Table 3
HIV-1 reverse transcriptase inhibition of compounds.

Sample	Inhibition percentage (%)
1	24.3 ± 1.7
1a	4.4 ± 0.3
1b	13.4 ± 0.8
1c	3.2 ± 0.1
1d	9.7 ± 0.8
Nevirapine (1 μM)	38.3 ± 2.5

Table 4
SARS-CoV-2 M^{pro} inhibition of compounds.

Compounds	Inhibition percentage (%)
1	71.1 ± 1.7
1a	46.7 ± 1.0
1b	20.6 ± 2.0
1c	32.5 ± 0.5
1d	22.9 ± 1.3
Lopinavir (1 μM)	47.7 ± 1.7

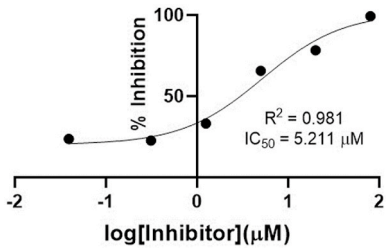

Fig. 3. The plot of M^{pro} inhibition percentage versus logarithm of concentrations of compound 1.

Samples of compound **1** at 10 different concentrations, prepared by 2-fold dilution from 80 to 0.2 μM, were used for IC_{50} determination. Compound **1** displayed remarkable potency against M^{pro}, evidenced by an IC_{50} value of 5.2 μM (Fig. 3).

2.5. Cytotoxicity and nitric oxide (NO) production inhibition assay

Compounds **1** and **1a**-**1d** were screened for cytotoxicity against three cancerous cell lines namely A549 (Lung carcinoma), and T47D (Breast cancer), and HepG2 (Hepatocarcinoma), and one non-cancerous L929 (mouse fibroblast) cell line. They were also evaluated for their anti-inflammatory activity. All compounds are inactive in both assays (see Tables S2 and S3).

Literature reviews indicated that diphenyl ethers and their halogenated derivatives have diverse biological activities such as antibacterial, alpha-glucosidase inhibition, antifungal, anti-inflammatory, and antiviral activities [23–27], which prompted us to screen the biological activities of compounds **1** and **1a**-**1d**. Unfortunately, most compounds were weak or inactive. The substituents of diphenyl ethers might play an important role in the biological activity rather than the etherified linkage. Regarding alpha-glucosidase inhibition, Devi and co-workers isolated two closely structure-related diphenyl ethers, parmetherines A and B, from the lichen *Parmotrema dilatatum* [27], possessing strong alpha-glucosidase inhibition. Comparison of the chemical structure between handelone (**1**) and parmetherines A and B indicated that the presence of 5-OH might decrease alpha-glucosidase inhibitory activity.

2.6. Molecular docking of 1

The binding energy of the interaction of compound **1** with M^{pro} protein was determined to be 67.60 kcal/mol. In Fig. 4, the 2D and 3D representations describe that **1** is mainly stabilized by interacting with M^{pro} through the formation a π–sulfur stacking with CYS145 and a π–Sigma stacking with MET165, while forming four H-bonds with LEU141, SER144, HIS163 and GLU166. Those interactions were visualized using PyMOL [28] and Discovery Studio Visualizer v21.1.0.20,298; https://www.3ds.com/products-services/biovia/).

3. Experimental

3.1. General experimental procedures

For nuclear magnetic resonance (NMR) and high-resolution electronspray ionization mass spectroscopic (HRESIMS) spectra, the Bruker Avance III and MicrOTOF-Q mass spectrometers were selected. The following deuterated solvents were used to record the NMR spectra (500 MHz for ^{1}H and 125 MHz for ^{13}C): $CDCl_3$, DMSO-d_6, and CD_3OD. Normal-phase and reverse-phase silica gel (Merck) were used for thin-layer chromatography (TLC). The Himedia silica gel 60 was utilized for the column chromatography (CC) procedure. Yeast *Saccharomyces cerevisiae* alpha-glucosidase enzyme (Sigma-Aldrich, EC3.2.1.20) and the positive control acarbose (Sigma-Aldrich, EC260-030-7), and Griess' reagent (Sigma-Aldrich, EC215-981-2) were utilized.

3.2. Lichen material

In March 2022, *Graphis handelii* material was gathered in Duc Trong District, Lam Dong Province. Dr. T.-P. G. Vo identified the scientific name with the voucher specimen (UE-L010) kept in the HCMUS Herbarium.

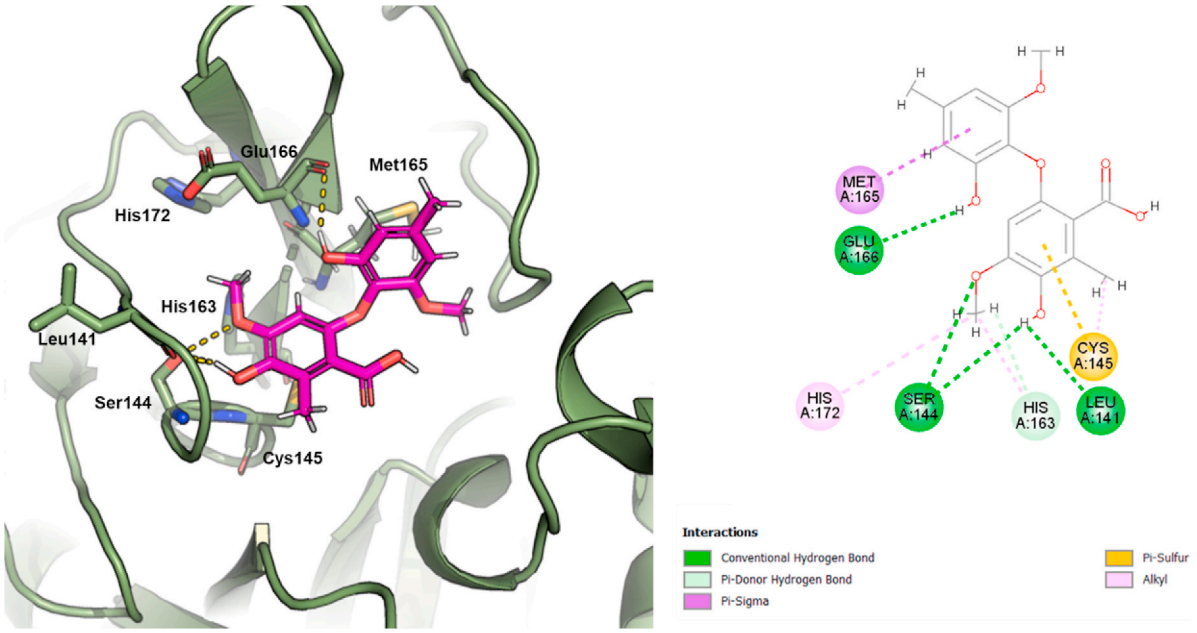

Fig. 4. The 2D and 3D binding mode of the M^{pro} protein with molecule **1** in the active site. Hydrogen bonds are represented as dashed green lines, and the key interacting residues are displayed in Ball and sticks style, while hydrophobic interactions are indicated by dashed yellow lines.

3.3. Mycobiont culture

The lichen mycobiont culture method was derived from a study previously reported by Do et al. (2022) [13]. Briefly, a small piece of mycobiont was inoculated on the surface of MY10 medium (malt extract 10 g, yeast extract 4 g, sucrose 100 g, agar 15 g, distilled water 1 L) in 100 mL-flasks. These flasks were incubated at 18 °C in the dark for 10 weeks. After cultivation, the medium was carefully removed, and the mycobiont colonies were harvested, then placed in an oven at 50 °C for drying. Lichen mycobiont was kept at Department of Biology, Ho Chi Minh City University of Education with the number UE-MY04.

3.4. Extraction and isolation

After being dried and ground, 35 g of biomass were extracted with EtOAc (10 × 300 mL, each 12 h) at room temperature. The collected EtOAc solution was concentrated to give 167 mg of the crude EtOAc extract. The extract was then chromatographed by a silica gel CC with a mobile phase as *n*-hexane-EtOAc-acetone (5:1:0.5, v/v/v) to provide five fractions GR1 to GR5. Purification of fraction GR1 (36 mg) using the silica gel CC method with an eluent being *n*-hexane-acetone-$CHCl_3$-EtOAc-water (12:1:1:1.5:0.05, v/v/v/v/v) to give three fractions GR1.1–1.3. Fraction GR1.2 (11 mg) was purified by reverse-phase C_{18} silica gel CC, eluted with acetone-water (3:1, v/v) to obtain two compounds **1** (8.1 mg) and **2** (2.7 mg). Fraction GR1.3 (22 mg) was rechromatographed to give 21 mg of compound **1**. Fraction GR5 (41 mg) was dissolved in 20 mL of chloroform, leaving a solid (8 mg) and a liquid (33 mg). Purification of the liquid part by silica gel CC gave 30 mg of compound **1**.

3.4.1. Handelone (1)

White amorphous powder; ^{1}H NMR and ^{13}C NMR in acetone-d_6: See Table S1. HRESIMS *m/z*: 315.0867 $[M–H_2O–H]^-$ (calcd for $C_{17}H_{15}O_6^-$, 315.0868).

3.5. General procedure to synthesize compounds 1a-1d

Handelone (**1** 20.0 mg, 0.06 mmol) and sodium bromide (6.18 mg, 0.06 mmol) were dissolved in 4.0 mL of acetic acid to gain a reaction mixture that further was added by 4 mL of 30% hydrogen peroxide (0.18 mmol). The reaction time was conducted at room temperature for 2 h. After stopping the reaction, neutralization (by Na_2CO_3) and liquid-liquid extraction [ethyl acetate-water (1:1, v/v), three times] were performed consecutively. The obtained organic layer were applied to silica gel CC, eluted with *n*-hexane-acetone-EtOAc-water (4:0.5:1:0.01, v/v/v) to obtain **1a** (4.6 mg, 18%) and **1b** (3.7 mg, 15%).

To obtain **1b** (8.65 mg, 35%) and **1c** (7.37 mg, 25%), a similar procedure was applied using 20 mg of **1**, 37.08 mg of NaBr (0.36 mmol), and 8.5 mL of H_2O_2 30% (0.36 mmol) dissolved in 4.0 mL of CH_3CO_2H: DMSO (1:1, v/v). To obtain **1d** (5.5 mg, 25%), 20 mg of **1**, 21.06 mg of NaCl (0.36 mmol), and 2.0 mL of H_2O_2 30% (0.06 mmol) were dissolved in 4.0 mL of CH_3CO_2H: DMSO (1:1, v/v) and the reaction was conducted under the similar procedure.

3.5.1. 6′-Bromohandelone (1a)

White amorphous powder; ^{1}H NMR and ^{13}C NMR in acetone-d_6: see Table 1. HRESIMS *m/z*: 413.0239 $[M+H]^+$ (calcd for $C_{17}H_{18}BrO_7^+$, 413.02359).

3.5.2. 2′-Bromohandelone (1b)

White amorphous powder; ^{1}H NMR and ^{13}C NMR in chloroform-*d*: see Table 1. HRESIMS *m/z*: 413.0271 $[M+H]^+$ (calcd for $C_{17}H_{18}BrO_7^+$, 413.02359).

3.5.3. 2′,6′-Dibromohandelone (1c)

White amorphous powder; ^{1}H NMR and ^{13}C NMR in chloroform-*d*: see Table 1. HRESIMS *m/z*: 490.9099 $[M+H]^+$ (calcd for $C_{17}H_{17}O_7Br_2^+$, 490.93410).

3.5.4. 2′,6′-Dichlorohandelone (1d)

White amorphous powder; ^{1}H NMR and ^{13}C NMR in chloroform-*d*: see Table 1. HRESIMS *m/z*: 403.0346 $[M+H]^+$ (calcd for $C_{17}H_{17}O_7Cl_2^+$, 403.03513).

3.6. Alpha-glucosidase inhibition

A method adapted from a previous study was used to determine the alpha-glucosidase inhibitory activity of the crude extract, fractions, and compounds **1** and **1a-d** [29]. Each sample was measured in triplicate at nine different concentrations surrounding the IC_{50} values, and the average values were used for further analysis.

3.7. M^{pro} inhibition assay

Fluorescence Resonance Energy Transfer (FRET) assay was used for screening compounds against M^{pro}. Working solution of M^{pro} and FRET substrate were prepared in a reaction buffer (20 mM Tris pH 7.5, 100 mM NaCl, 2 mM DTT, 0.4 mM EDTA). Compounds **1** and **1a-1d** were prepared in a buffer with a similar composition to the reaction buffer, but without DTT. The assay was conducted in a 384-well black microplate with a final reaction volume of 25 μL per well. First, 10 μL of reaction buffer was added to each well, followed by 5 μL of 3 μM M^{pro}. Compounds were added to each well to achieve the final concentration of 10 μM. After being thoroughly mixed, the mixture underwent a 10-min incubation period at room temperature. Next, 5 μL of FRET substrate were added at the final concentration of 40 μM. The fluorescence intensity (excitation/emission, 340 nm/430 nm) was immediately measured in kinetic mode at 1 min intervals for 30 min using an Infinite 200 Pro multimode plate reader (Tecan, USA). The readings of reaction without inhibitor were used as the control for calculation of the inhibition percentage of compounds. The reaction has no inhibitors and M^{pro} enzyme was served as blank. The M^{pro} inhibition percentage of compounds was determined through the following equation: $\%I = (1 - \frac{S_s - S_b}{Sc - Sb}) * 100$, where S_S was the slope of the kinetic reaction with inhibitor, S_c was the slope of the kinetic reaction without inhibitor, S_b was the enzymatic of blank.

For IC_{50} determination, a total of 10 concentrations from 80 μM to 0.2 μM was prepared via 2-fold serial dilution. The IC_{50} values of compounds **1** and **1a-1d** were determined by analyzing dose-inhibition curves generated through nonlinear regression with a variable slope in GraphPad Prism 8.

3.8. HIV-1 reverse transcriptase inhibition assay

The Poly(A) ribonucleotide template and Oligo $d(T)_{16}$ primer was annealed by adding 2.5 μL of template 1 mg/mL and 2.5 μL of primer 50 μg/mL into a sterile tube, followed by incubation at room temperature for 1 h. After that, 995 μL of polymerization buffer (60 mM Tris-HCl pH 8.1, 60 mM KCl, 8 mM $MgCl_2$, 13 mM DTT and 100 μM dTTP) was added into the tube. The assay for screening of compounds that inhibit HIV-1 reverse transcriptase was performed in a 96-well black plate (25 μL/well). First, 3 μL of reaction buffer (20 mM Tris pH 7.5, 100 mM NaCl, 2 mM DTT, 0.4 mM EDTA) were dispensed into each well, followed by 15 μL of template primer mixture. The next step involved adding compounds in DMSO to a final concentration of 10 μM. Next, 5 μL of HIV-1 reverse transcriptase solution (25 nM) was introduced to the reaction mixture. The mixture underwent a 30-min incubation period at room temperature after being well mixed. Next, the reaction was inhibited by adding 2 μL of 0.2 M EDTA to each well. After that, 173 μL of PicoGreen dye in 1X TE buffer was added. The fluorescence at 485 nm excitation and 535 nm emission was immediately measured in endpoint mode using an Infinite 200 Pro multimode plate reader (Tecan, USA). The reaction without inhibitor (2 μL of DMSO instead) was served as the control. For the blank, 2 μL of inhibitor was replaced by 2 μL of DMSO, and the reaction was pre-treated with 2 μL of 0.2 M EDTA before the addition of enzyme. Nevirapine 1 μM was used as positive control. The inhibition percentage was calculated as the following equation: $\%I = (1 - \frac{F_s - F_b}{Fc - Fb}) * 100$, where Fs: fluorescence intensity of the samples, Fc: fluorescence intensity of control, Fb: Fluorescence intensity of blank.

3.9. Cytotoxicity assay

Compounds **1** and **1a-1d** were evaluated their cytotoxicity against selected cancerous cell lines: A549 (lung carcinoma), T47D

(breast cancer), and HepG2 (hepatocarcinoma) (gift from Prof. Palaga's lab at Chulalongkorn University, Thailand), and one non-cancerous L929 (mouse fibroblast) cell line. MTT method was modified using a similar protocol described previously [30]. In 96-well plates, above-mentioned cells were seeded (each well contained 10^4 cells) then incubated for 24 h (the tested condition: 37 °C in 5%-CO_2 humidified air). Next, two different concentrations of each compound (10 and 50 μM) were added to each prepared well of 96-well plates. The incubation continued under the same conditions for next 48 h. Then, 5 mg/mL of 3-(4,5-dimethylthiazol-2-yl)-2, 5-diphenylte-trazolium bromide in PBS (so-called MTT solution) was added to the wells and the test was continued for another 3 h. The medium was then discarded and 200 μL of DMSO was pipetted to each well and mixed. A Scientific Varioskan LUX multimode microplate reader was utilized to record the absorbance at 570 nm. The positive control cisplatin, a common anticancer drug, was used (concentration: 10 and 50 μM). Each compound was measured in triplicate.

3.10. Nitric oxide (NO) production inhibition assay

Compounds **1** and **1a-1d** were evaluated for the nitric oxide (NO) inhibitory activity following the same method [30]. A Scientific Varioskan LUX multimode microplate reader was utilized to record the absorbance at 540 nm. The assay was conducted in triplicate and repeated in three independent experiments. 5 μM of the positive control Bay 11–7082 was acquired, which showed the % NO inhibition ±SD equal to 72.5 ± 3.9 % with % Cell viability ±SD equal to 82.7 ± 5.3.

3.11. Molecular docking

The three-dimensional crystal structure of the main protease (M^{pro}) (PDB code: 6XBG) complexed with the inhibitor UAW246 was obtained from the Protein Data Bank [31]. The M^{pro} protein was prepared using the protein preparation wizard within the GOLD setup window [32]. To define the binding cavity of the receptor, we selected all amino acids located within a 10 Å radius of the UAW246 reference ligand in 6XBG. Molecule **1** was then docked into the binding site of the SARS-CoV-2 M^{pro} to predict binding poses for the hit molecule. The docking search employed 50 Genetic Algorithm runs with the Goldscore scoring function in the GOLD CCDC program. The binding interactions of the best poses of the compound were determined using the Discovery Studio Visualizer v21.1.0.20,298; https://www.3ds.com/products-services/biovia/) and PyMOL programs [28].

3.12. Computational details

Two isomers **I** and **II** of compound **1** were optimized using the B3LYP/6-311g(d,p) method in Schrodinger's Jaguar software. The calculations were conducted under DFT theory, considering NMR shielding constants in the gas phase. Then, the DP4 Java code, available from the Goodman lab (http://wwwjmg.ch.cam.ac.uk/tools/nmr/DP4/), was employed to compare the predicted chemical shifts with the experimentally obtained values. The method followed the previous reports [20,21]. Coordinations of two isomers were shown in Supporting information.

4. Conclusions

In this study, a new compound handelone (**1**) and a known compound xylarinic acid A (**2**) were isolated from the cultured mycobiont of the lichen *Graphis handelii*. Synthetic compounds 6′-bromohandelone (**1a**), 2′-bromohandelone **(1b)**, 2′,6′-dibromo-handelone **(1c)**, and 2′,6′-dichlorohandelone (**1d**) were prepared. Compound **1** showed good activity against M^{pro} with an IC_{50} value of 5.2 μM.

Data availability statement

Data included in the article and supplementary material.

CRediT authorship contribution statement

Thi-Minh-Dinh Tran: Methodology, Investigation, Funding acquisition, Data curation, Conceptualization. **Chanat Aonbangkhen:** Investigation. **Thuc-Huy Duong:** Writing – review & editing, Writing – original draft, Visualization, Methodology, Investigation, Formal analysis, Conceptualization. **Thu-Hoang-Mai Nguyen:** Investigation, Formal analysis. **Minh-Truong-Tho Ho:** Methodology, Investigation, Data curation. **Warinthorn Chavasiri:** Methodology, Investigation, Formal analysis. **Sutthida Wongsuwan:** Investigation. **Jaruwan Chatwichien:** Investigation. **Thi-Phi Giao Vo:** Methodology, Investigation. **Ngoc-Hong Nguyen:** Methodology, Investigation. **Duangnapa Kiriwan:** Formal analysis, Data curation. **Kiattawee Choowongkomon:** Writing – review & editing, Funding acquisition, Conceptualization.

Declaration of competing interest

The authors declare that they have no known competing financial interests or personal relationships that could have appeared to influence the work reported in this paper.

Acknowledgement

This research is funded by Ho Chi Minh city University of Education Foundation for Science and Technology under grant number CS2022.19.13 TĐ. This work was financially supported by the Office of the Ministry of Higher Education, Science, Research and Innovation; and the Thailand Science Research and Innovation through the Kasetsart University Reinventing University Program 2022. Kasetsart University Research and Development Institute (KURDI) Bangkok, Thailand, KURDI (FF(KU)) 51.67) is also acknowledged.

Appendix A. Supplementary data

Supplementary data to this article can be found online at https://doi.org/10.1016/j.heliyon.2024.e25763.

References

[1] D.H. Le, Y. Takenaka, N. Hamada, T. Tanahashi, Eremophilane-type sesquiterpenes from cultured lichen mycobionts of Sarcographa tricosa, Phytochemistry 91 (2013) 242–248, https://doi.org/10.1016/j.phytochem.2012.01.009.
[2] Y. Takenaka, N. Hamada, T. Tanahashi, Monomeric and dimeric dibenzofurans from cultured mycobionts of Lecanora iseana, Phytochemistry 66 (2005) 665–668, https://doi.org/10.1016/j.phytochem.2004.12.031.
[3] Y. Takenaka, N. Hamada, T. Tanahashi, Biosynthetic origin of graphenone in cultured lichen mycobionts of Graphis handelii, Zeitschrift Für Naturforschung C 63 (2008) 565–568, https://doi.org/10.1515/znc-2008-7-817.
[4] Y. Takenaka, N. Hamada, T. Tanahashi, Aromatic compounds from cultured lichen mycobionts of three Graphis species, Natural Product Updates 83 (2011) 2157–2164.
[5] T. Tanahashi, Y. Takenaka, N. Nagakura, N. Hamada, 6H-Dibenzo[b,d]pyran-6-one derivatives from the cultured lichen mycobionts of Graphis spp. and their biosynthetic origin, Phytochemistry 62 (2003) 71–75, https://doi.org/10.1016/S0031-9422(02)00402-8.
[6] L.Y. Sun, Z.L. Liu, T. Zhang, S.B. Niu, Z.T. Zhao, Three antibacterial naphthoquinone analogues from cultured mycobiont of lichen Astrothelium sp, Chinese Chemical Letters 21 (2010) 842–845, https://doi.org/10.1016/j.cclet.2010.03.024.
[7] K. Kinoshita, Y. Yamamoto, K. Takatori, K. Koyama, K. Takahashi, K. Kawai, I. Yoshimura, Fluorescent compounds from the cultured mycobiont of Amygdalaria panaeola, J. Nat. Prod. 68 (2005) 1723–1727, https://doi.org/10.1021/np040239j.
[8] H. Miyagawa, N. Hamada, M. Sato, T. Eeno, Pigments from the cultured lichen mycobionts of Graphis scripta and G. desquamescens, Phytochemistry 36 (1994) 1319–1322, https://doi.org/10.1016/S0031-9422(00)89659-4.
[9] P. Pittayakhajonwut, V. Sri-indrasutdhi, A. Dramae, S. Lapanun, R. Suvannakad, M. Tanticharoen, Graphisins A and B from the lichen Graphis tetralocularis, Aust. J. Chem. 62 (2009) 389–391.
[10] V.G. Vo, H.-D. Le, T.-N. Tran, N.-H. Nguyen, T.-P.G. Vo, J. Sichaem, V.-K. Nguyen, T.-H. Duong, A new eremophilane-sesquiterpene from the cultured lichen mycobiont of *Graphis* sp, Natural Product Research 36 (2022) 319–325, https://doi.org/10.1080/14786419.2020.1779717.
[11] Y. Takenaka, S. Taguchi, D.H. Le, N. Hamada, T. Tanahashi, 3,4-dihydro-2H, 5H-pyrano[3, 2-c] chromene and benzophenone derivatives from cultured lichen mycobionts of Vietnamese Graphis sp, Heterocycles 87 (2013) 2651–2657.
[12] T. Tanahashi, Y. Takenaka, N. Nagakura, N. Hamada, 2, 3-Dialkylchromones from mycobiont cultures of the lichen Graphis scripta, Heterocycles 53 (2000) 1589–1593.
[13] T.-H. Do, T. Aree, H.-H. Nguyen, H.-C. Nguyen, T.-P.G. Vo, N.-H. Nguyen, T.-H. Duong, Two new guaiane-sesquiterpenes from the cultured lichen mycobiont of Diorygma pruinosum, Phytochemistry Letters 52 (2022) 59–62.
[14] T.-H. Duong, H.-H. Nguyen, T.-T. Le, T.-N. Tran, J. Sichaem, T.-T. Nguyen, T.-P. Nguyen, D.-T. Mai, H.-H. Nguyen, H.-D. Le, Subnudatones A and B, new trans-decalin polyketides from the cultured lichen mycobionts of Pseudopyrenula subnudata, Fitoterapia 142 (2020) 104512, https://doi.org/10.1016/j.fitote.2020.104512.
[15] Y.-W. Jang, I.-K. Lee, Y.-S. Kim, S. Lee, H.-J. Lee, S.H. Yu, B.-S. Yun, Xylarinic acids A and B, new antifungal polypropionates from the fruiting body of xylaria polymorpha, J Antibiot 60 (2007) 696–699, https://doi.org/10.1038/ja.2007.89.
[16] Y. Chen, L.-T. Sun, H.-X. Yang, Z.-H. Li, J.-K. Liu, H.-L. Ai, G.-K. Wang, T. Feng, Depsidones and diaryl ethers from potato endophytic fungus Boeremia exigua, Fitoterapia 141 (2020) 104483, https://doi.org/10.1016/j.fitote.2020.104483.
[17] T.-H. Duong, W. Chavasiri, J. Boustie, K.-P.-P. Nguyen, New meta -depsidones and diphenyl ethers from the lichen Parmotrema tsavoense (krog & swinscow) krog & swinscow, Parmeliaceae, Tetrahedron. 71 (2015) 9684–9691, https://doi.org/10.1016/j.tet.2015.06.107.
[18] C. Zhang, M. Wang, P. Lin, M. Zhang, Z. Wang, L. Xu, A new bibenzyl compound from Dendrobium gratiosissmum, J. Indian Chern. Soc. 84 (2007) 714–716.
[19] R.A.C. Souza, B.A. Ferreira, F.B.R. de Moura, T. da Costa Silva, F. Cavalcanti, E. de F. Franca, R.M.F. de Sousa, J. de L. Febronio, J.H.G. Lago, F. de A. Araújo, A. de Oliveira, Dehydrodieugenol B and hexane extract from Endlicheria paniculata regulate inflammation, angiogenesis, and collagen deposition induced by a murine sponge model, Fitoterapia 147 (2020) 104767, https://doi.org/10.1016/j.fitote.2020.104767.
[20] T.-H. Duong, M.A. Beniddir, G. Genta-Jouve, T. Aree, M. Chollet-Krugler, J. Boustie, S. Ferron, A. Sauvager, H.-H. Nguyen, K.-P.-P. Nguyen, W. Chavasiri, P. Le Pogam, A.C. Tsavoenones, Unprecedented polyketides with a 1,7-dioxadispiro[4.0.4.4]tetradecane core from the lichen *Parmotrema tsavoense*, Org. Biomol. Chem. 16 (2018) 5913–5919, https://doi.org/10.1039/C8OB01280F.
[21] T.-H. Duong, X.-P. Ha, W. Chavasiri, M.A. Beniddir, G. Genta-Jouve, J. Boustie, M. Chollet-Krugler, S. Ferron, H.-H. Nguyen, B.M. Yamin, B.-L.-C. Huynh, P. Le Pogam, K.-P.-P. Nguyen, A.-C. Sanctis, Three racemic procyanidin analogues from the lichen *Parmotrema sancti-angelii*: sanctis A-C: three racemic procyanidin analogues from the lichen *Parmotrema sancti-angelii*, Eur. J. Org. Chem. 2018 (2018) 2247–2253, https://doi.org/10.1002/ejoc.201800202.
[22] T.-H. Do, T.-H. Duong, H.T. Nguyen, T.-H. Nguyen, J. Sichaem, C.H. Nguyen, H.-H. Nguyen, N.P. Long, Biological activities of lichen-derived monoaromatic compounds, Molecules 27 (2022) 2871, https://doi.org/10.3390/molecules27092871.
[23] Z.K. Sweeney, J.J. Kennedy-Smith, J. Wu, N. Arora, J.R. Billedeau, J.P. Davidson, J. Fretland, J.Q. Hang, G.M. Heilek, S.F. Harris, D. Hirschfeld, P. Inbar, H. Javanbakht, J.A. Jernelius, Q. Jin, Y. Li, W. Liang, R. Roetz, K. Sarma, M. Smith, D. Stefanidis, G. Su, J.M. Suh, A.G. Villaseñor, M. Welch, F. Zhang, K. Klumpp, Diphenyl ether non-nucleoside reverse transcriptase inhibitors with excellent potency against resistant mutant viruses and promising pharmacokinetic properties, ChemMedChem 4 (2009) 88–99, https://doi.org/10.1002/cmdc.200800262.
[24] K.S. Singh, A. Singh, Chemical diversities, biological activities and chemical synthesis of marine diphenyl ether and their derivatives, Journal of Molecular Structure 1265 (2022) 133302, https://doi.org/10.1016/j.molstruc.2022.133302.
[25] L. Schmitt, I. Hinxlage, P.A. Cea, H. Gohlke, S. Wesselborg, 40 Years of research on polybrominated diphenyl ethers (PBDEs)—a historical overview and newest data of a promising anticancer drug, Molecules 26 (2021) 995, https://doi.org/10.3390/molecules26040995.
[26] K. Sadorn, S. Saepua, N. Bunbamrung, N. Boonyuen, S. Komwijit, P. Rachtawee, P. Pittayakhajonwut, Diphenyl ethers and depsidones from the endophytic fungus Aspergillus unguis BCC54176, Tetrahedron 105 (2022) 132612, https://doi.org/10.1016/j.tet.2021.132612.
[27] A.P. Devi, T.-H. Duong, S. Ferron, M.A. Beniddir, M.-H. Dinh, V.-K. Nguyen, N.-K.-T. Pham, D.-H. Mac, J. Boustie, W. Chavasiri, P.L. Pogam, Salazinic acid-derived depsidones and diphenylethers with α-glucosidase inhibitory activity from the lichen Parmotrema dilatatum, Planta Med 86 (2020) 1216–1224.

[28] S. Yuan, H.C.S. Chan, S. Filipek, H. Vogel, PyMOL and inkscape bridge the data and the data visualization, Structure 24 (2016) 2041–2042, https://doi.org/10.1016/j.str.2016.11.012.
[29] T.-H. Duong, T.-X.-H. Hang, P.L. Pogam, T.-N. Tran, D.-H. Mac, M.-H. Dinh, J. Sichaem, α-Glucosidase inhibitory depsidones from the lichen Parmotrema tsavoense, Planta Med 86 (2020) 776–781.
[30] E.R. Sukandar, S. Kaennakam, S. Wongsuwan, J. Chatwichien, S. Krobthong, Y. Yingchutrakul, T. Mahatnirunkul, F. Mulya, V. Parasuk, D.J. Harding, P. Poldorn, T. Rungrotmongkol, S. Tip-pyang, C. Aonbangkhen, W. Chavasiri, Schomburginones A–J, geranylated benzophenones from the leaves of Garcinia schomburgkiana and their cytotoxic and anti-inflammatory activities, Phytochemistry 211 (2023) 113701, https://doi.org/10.1016/j.phytochem.2023.113701.
[31] J. Cole, J. Willem M. Nissink, R. Taylor, Protein,ÄìLigand docking virtual screening with GOLD, in: J. Alvarez, B. Shoichet (Eds.), Virtual Screening in Drug Discovery, CRC Press, 2005, pp. 379–415, https://doi.org/10.1201/9781420028775.ch15.
[32] M.D. Sacco, C. Ma, P. Lagarias, A. Gao, J.A. Townsend, X. Meng, P. Dube, X. Zhang, Y. Hu, N. Kitamura, B. Hurst, B. Tarbet, M.T. Marty, A. Kolocouris, Y. Xiang, Y. Chen, J. Wang, Structure and inhibition of the SARS-CoV-2 main protease reveal strategy for developing dual inhibitors against M ^{pro} and cathepsin L, Sci. Adv. 6 (2020), https://doi.org/10.1126/sciadv.abe0751 eabe0751.